Approximate *ab initio* calculations of electronic structure of amorphous silicon

M. Durandurdu, D. A. Drabold, and N. Mousseau

Department of Physics and Astronomy, Condensed Matter and Surface Science Program, Ohio University, Athens, Ohio 45701-2979

(Received 7 June 2000)

We report on *ab initio* calculations of electronic states of two large and realistic models of amorphous silicon generated using a modified version of the Wooten-Winer-Weaire algorithm and relaxed, in both cases, with a Keating and a modified Stillinger-Weber potentials. The models have no coordination defects and a very narrow bond-angle distribution. We compute the electronic density-of-states and pay particular attention to the nature of the band-tail states around the electronic gap. All models show a large and perfectly clean optical gap and realistic Urbach tails. Based on these results and the extended quasi-one-dimensional stringlike structures observed for certain eigenvalues in the band tails, we postulate that the generation of model *a*-Si without localized states might be achievable under certain circumstances.

I. INTRODUCTION

Amorphous silicon is an important material because of its applications in electronic and photoelectronic industry and its role as the archetype of disordered system. Applications of the material depend strongly on the nature of electron states near the Fermi level. Therefore there have been very large number of studies of electron states of *a*-Si.[1–4]

The major hurdle for getting the right electronic picture of *a*-Si is the limited availability of high quality structural models. Models generated with molecular dynamics (MD) generally show an unrealistic defect concentration and barely exhibit an optical gap. The presence of a large number of defects in close proximity in energy and real space (inevitable in a small supercell model) implies delocalization of the defect wave functions. This unphysical delocalization then impacts any calculation of transport or photostructural change. It is not even obvious that structural and dynamical characteristics of such a model are reliable. This is because some of the artificially extended defect states are *occupied*. The generation of defect-free models is therefore fundamental to the understanding of the role of realistic defects and nature of the band tails in amorphous semiconductors.

In this paper, we compute electron eigenstates of 2 large 1000-atom realistic models of *a*-Si using an approximate *ab initio* scheme. This is close to the maximum size that can be treated with *ab initio* MD at present. These models were prepared using an improved version of the Wooten-Winer-Weaire (WWW) algorithm[5] and were each relaxed with both a Keating[6] and a modified Stillinger-Weber potential,[7] for a total of four different configurations. All the configurations are perfectly fourfold coordinated with a narrow bond-angle distribution, almost two degrees below the next best available numerical models and on a par with experimental values.[8] Because of the low density of strain in the network, the electronic density-of-states (EDOS) of these models also show a clean gap, with no state extending beyond the Urbach tails. To our knowledge, these are the first models of *a*-Si to show a perfect wide gap. Analyzing the states in the band tails, we find that one of the models has only very weakly localized electronic states, leading to extended one-dimensional (1D) stringlike structures while the three others show a significant degree of localization near the band edge. The results obtained generally confirm a recent study of *a*-Si.[1]

II. METHODOLOGY

The models used here were generated by Barkema and Mousseau[5] using a significantly improved version of the WWW algorithm.[9] The details of the preparation are reported in Ref. 5 and we just give a brief review here. Two independently generated 1000-atom models of *a*-Si were created.

Atoms are first packed randomly in a box, at crystalline density, with the single constraint that no two atoms be closer than 2.3 Å. A connectivity table is then constructed by constructing a loop that passes exactly twice through each atom. The network is then relaxed, using the fixed list of neighbors and a Keating potential. These steps ensure that the initial state has no trace of crystallinity. The models are then relaxed in a series of WWW moves and additional massaging, using the accelerated algorithm discussed in Ref. 5. The flexibility of such static methods allows the creation of high quality amorphous network with relatively little computational effort.

The two independent models were finally relaxed, at zero pressure, with both a Keating and a modified Stillinger-Weber (SW) potential, leading to four different configurations: $K1$ and $mSW1$, and $K2$ and $mSW2$. Both $K1$ and $mSW1$ share a common topology but present slight differences regarding structural and electronic properties, including density and strain. The same applies, of course, to $K2$ and $mSW2$. All supercells have perfect fourfold coordinations with a narrow bond-angle distribution $\Delta\theta = 9.21$, 9.20, 9.70, and 9.77 for $K1$, $K2$, $mSW1$, and $mSW2$ supercells, respectively.

The use of two potentials is made necessary because it is not numerically reasonable to relax a 1000-atom cell *ab initio*. In order to assess the error generated by studying the electronic properties of models structurally optimized for empirical potential, we tested the total energy per atom with a 216-atom model of *a*-Si. The model was relaxed with both the modified Stillinger-Weber potential and the FIREBALL96

TABLE I. Total energy per atom, their energy difference with c-Si, and the density of the models.

Model	$K1$	$K2$	mSW1	mSW2
E_{tot}^a/atom (eV)	-107.765	-107.698	-107.810	-107.827
(E_{tot}^a/atom-E_{tot}^c/atom)(eV)	0.229	0.296	0.1841	0.167
ρ(gr cm^{-3})	2.335	2.436	2.200	2.196

program of Demkov et $al.$,[10] which generalizes the nonself-consistent minimal basis Harris functional local-density approximation scheme of Sankey and Niklewski.[11] This program has been successfully applied in a wide range of amorphous systems a-Si,[2] a-GaN,[12] a-C,[13] and GeSe$_2$.[14]

In order to characterize the localized electronic states, we define the Mulliken charge,[15] $Q(n,E)$, for atom n associated with the eigenvalue E. This charge can then be used as a measure of the localization of a given state

$$Q_2(E) = N \sum_{n=1}^{N} Q(n,E)^2, \qquad (1)$$

where N is the number of atoms in a supercell. For a uniformly extended state, $Q_2(E)$ is 1, while it is N for a state perfectly localized on a single atom.

In amorphous and glassy substances, $Q_2(E)$ cannot be unity since the weight of even the most delocalized electronic states will fluctuate from site to site. This does not mean that the states are localized in the sense of charge falling off exponentially in an infinite model; it merely reflects the disordered nature of the model. In any finite sample, moreover, it is virtually impossible to define exactly where the band tail ends.

III. RESULTS AND DISCUSSIONS

The total energy per atom, E_{tot}^a/atom, the density of the models, and their energy difference with c-Si(E_{tot}^c/atom$=-107.994$ eV) are given in Table I. The energy difference of mSW1 and mSW2 supercells is in good agreement with a study of nonorthogonal tight-binding model.[16] However, the difference is a factor of 2 higher than an experimental result 0.0977 eV, as extrapolated to 0 K from the measurement at 960 K using the specific heat listed in that work.[17]

The configurational energy of the $K1$ and $K2$ models is significantly higher than that of mSW1 and mSW2. This is due to the fact that the optimal density of amorphous models relaxed with Keating potential is slightly higher than that of the crystal ($\rho=2.243$ g/cm^3) while the modified Stillinger-Weber potential favors a density slightly lower, in agreement with experiment.

The EDOS of the four supercells is given in Fig. 1(a). The energy bands are rather broad with band tails going into the gap. The disordered nature of a-Si is responsible for the band tails, especially valence tail and the conduction tails are dominated by thermal rather than structural disorder.[18] The region around the electronic gap is shown in more detail in Fig. 1(b). The absorption edge, extending into the gap, is called an Urbach edge and should show an exponential decay. Figs. 1(c) and 1(d) present a fit of this function, $\rho(E) \propto \exp(-E/E_0)$, for $K1$ and mSW2. In both cases, the fit is reasonable with a similar fitting parameter, $E_0=0.185$ eV and $E_0=0.205$ eV, respectively. This is in agreement with previous calculations.[1]

The optical gap of the cells is summarized in Table II. Comparing to the gap of the crystalline model, 1.55 eV, all models exhibit a rather wide and perfectly clean optical gap between 0.8 and 1.35 eV. Unexpectedly, the two best configurations from an energetic point of view, mSW1 and mSW2, show a narrower gap. This phenomenon appears to be directly related to the density of the cells. The modified Stillinger-Weber potential leads to a density slightly lower than that of c-Si, creating a small gap with a higher density of localized states on the edges. For a unique topology, density and the details of relaxation can therefore play a major role in determining the electronic properties around the gap.
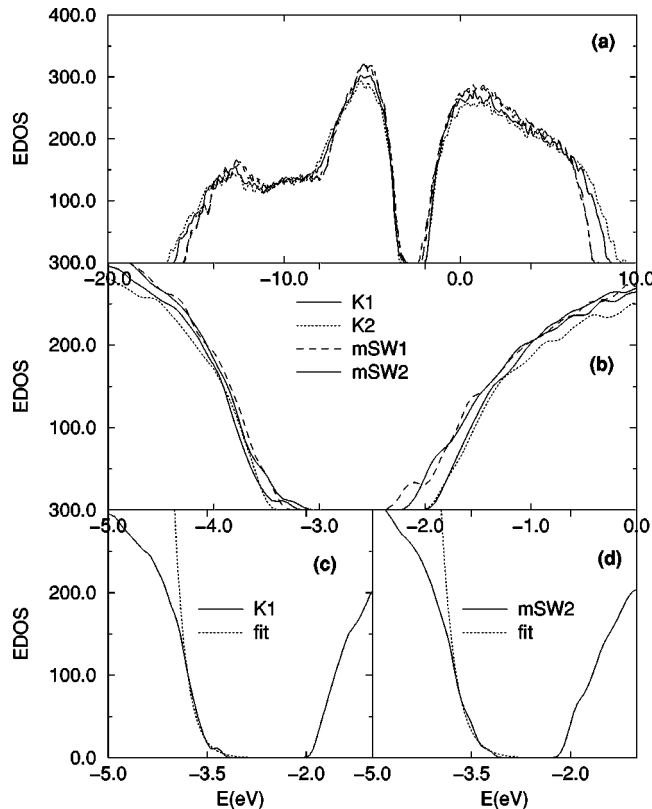
FIG. 1. (a) Total electronic density-of-states (EDOS). (b) Electronic density-of-state in the band-gap region. (c) and (d) The exponential fit of $K2$ and mSW2 model, respectively.

TABLE II. The optical gap of the models.

Model	$K1$	$K2$	mSW1	mSW2
Gap (eV)	1.15	1.35	0.85	0.8
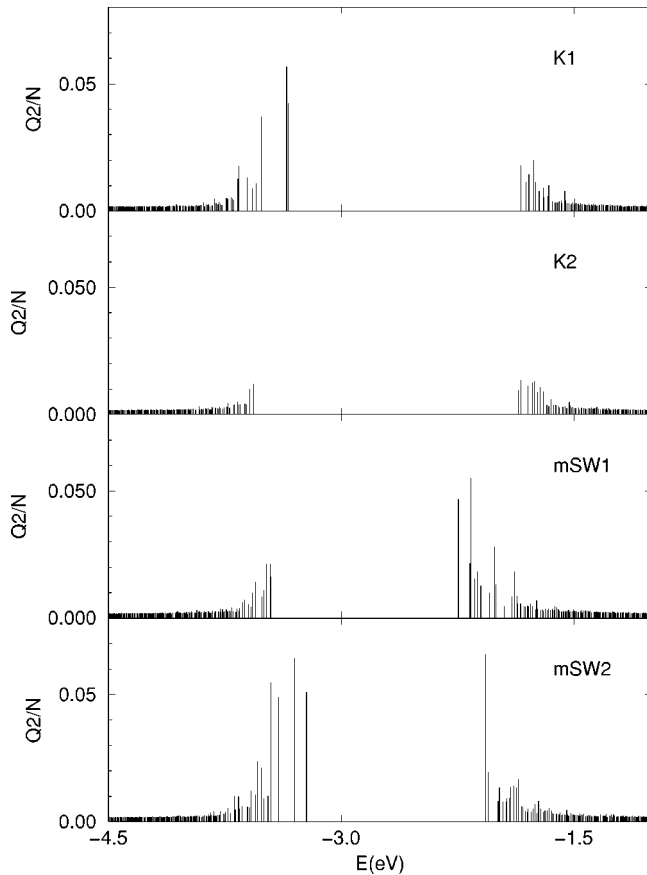
FIG. 2. Electronic eigenstates in the band-gap region. The position of vertical bars represents the eigenvalues of the electronic eigenstates and height of the bars is the spatial localization $Q_2(E)$.

FIG. 3. Spatial character of the local-to-extended transition in mSW1. For a given eigenstate, the electron charge density depicted according to the four level gray scale. Each atom shown according to the fraction of total charge: very dark ($\geq 10\%$), less dark ($\geq 5\%$), light ($\geq 1\%$), and white ($\leq 1\%$) such that at least 35% of the total charge is shown. The upper-left panel is a localized (midgap) state with $E = -3.226$ eV and $Q_2(E) = 0.05105N$. The upper-right and lower-left panel are less extended valence states with $E = -3.588$ eV, $Q_2(E) = 0.0057N$, $E = -3.785$ eV, and $Q_2(E) = 0.0027N$, respectively. The lower-right panel is an extended valence state with $E = -4.196$ eV and $Q_2(E) = 0.0018N$.

The rms static charge deviation of the models ranges between $0.042e - 0.051e$. These values are less than the experimental value of $0.11e$ (Ref. 19) and another first-principles calculation result of $0.14e$.[20] The smaller deviations can be attributed to both ambiguity associated with the basis sets, and differences between the models analyzed. It is perhaps unsurprising that these defect-free models show less fluctuation.

The localization of the electronic states, $Q_2(E)$, defined in Eq. (1) for the four models is shown in Fig. 2. Each spike represents a single electronic eigenvalue. The larger the $Q_2(E)$ for a state, the more spatially localized it is. As expected, the more localized states are on the edge of the band, where mixing is minimum. They extend within a range of about 0.3 to 0.6 eV on each side of the gap into the valence and conduction tail. Depending on the model, the $Q_2(E)$ peaks between $0.012N$ and $0.064N$. These values of localization are small compared to Bethe lattice calculations that show a $Q_2(E)$ of up to $0.70N$.[21] Nevertheless, all these states cannot be considered totally delocalized.

Comparing with previous work,[2] we would say that a $Q_2(E)$ greater than a tenth or so of N, is localized. Using this definition, we would say that $K1$, SW1, and SW2 show some degree of localization in either the valence or the conduction bands or both. The exact reason for the nature of the localization is not clear at the moment. Surprisingly, there is essentially no trace of localization in the EDOS of $K2$. Based on the width of the optical gap, this result was to be

expected. However, $K2$ is also the most energetic of the four configurations considered. Localized states could therefore help reduce the overall configurational energy of a structure by concentrating the strain on a few atoms only. This remarkable result also raises an important question: *Can* a-*Si exist with no localized state whatsoever?* Although we lack experimental and theoretical support, based on the current paper, we believe that it is possible to generate a model of a-Si with no coordination defect, a narrow bond-angle distribution, and absolutely no localized state representing the *ideal a*-Si model.

To examine the spatial structure of an electronic eigenstate, we visualize the states in two steps: (i) the electron charge associated with each atom site is calculated for a given electronic eigenstate, (ii) each atom is then drawn in one of the four levels of the gray scale according to amount of charge associated with it. Very dark atoms are strongly localized sites that contribute more than 10% of total charge each, less dark atoms are sites that contribute more than 5%, light atoms are sites that contribute more than 1% each, and white atoms contribute the rest in Fig. 3. For clarity, the atoms that contribute the least charge for the given eigenstates are omitted in the figure.

The localization of four chosen valence states is given in Table III. The states evolve from a localized (midgap) state to an extended valence state. We visualize these states for SW2 in Fig. 3 and in color on the WWW.[22] The reason for selecting this model is that SW2 shows more localization

TABLE III. The measure of localization [four chosen valence states from a localized state (ls), to less extended states (lexs) and, to an extended state (exs) of the models].

Model	$Q_2(E)$(ls)	$Q_2(E)$(lexs)	$Q_2(E)$(lexs)	$Q_2(E)$(exs)
$K1$	0.0422N	0.00489N	0.0024N	0.0018N
$K2$	0.0119N	0.0028N	0.002N	0.0016N
mSW1	0.016N	0.0062N	0.0024N	0.0018N
mSW2	0.051N	0.005N	0.0027N	0.0018N

than the others. The charge is confined to a cluster or clusters of atoms near to a recognizable structural distortion (small band angle deviation or stretched bonds) as in the midgap states as shown in the upper-left panel of Fig. 3. The clusters have extended 1D stringlike character for certain eigenstates in the band tails. As the energy is turned from the localized states to the valence states, the cluster size increases smoothly. The meaning is that the spatial character of these eigenstates goes through a so-called Anderson[23] (localized to extended) transition. Such a behavior in a-Si was recently obtained by Dong and Drabold,[1] and they proposed that this phenomenon could be explained by the resonant tunneling between cluster with similar electronic energies. Although the extended states are important in deciding the optical properties of amorphous semiconductors, hopping transport mainly occurs between midgap states.

IV. CONCLUSIONS

Electronic properties of four 1000-atom models of a-Si generated using the modified version of the WWW algorithm have been analyzed using an approximate *ab initio* tech-nique. All models exhibit a wide totally clean gap without states and exponential band tails. The models show a relatively weak localization near both the valence- and the conduction-band edges. The midgap states are slightly Anderson localized and the states are extended as we move into the valence- or conduction-band tails. It appears that an *ideal* model of a-Si would show no localized state at all along with a narrow bond-angle distribution and a perfectly fourfold coordination. Although the modified Stillinger-Weber potential is a more realistic interaction potential that does not require a preset list of neighbors, the results show that the Keating potential is electronically better than the modified Stillinger-Weber potential. This feature remains to be investigated.

[1] J. Dong and D.A. Drabold, Phys. Rev. Lett. **80**, 1928 (1998).

[2] P.A. Fedders, D.A. Drabold, and S. Nakhmanson, Phys. Rev. B **58**, 15 624 (1998).

[3] D.A. Drabold and P.A. Fedders, Phys. Rev. B **60**, R712 (1999).

[4] D.A. Drabold, J. Non-Cryst. Solids **266**, 211 (2000).

[5] G. T. Barkema and N. Mousseau, Phys. Rev. B **62**, 4985 (2000).

[6] P.N. Keating, Phys. Rev. **145**, 637 (1966).

[7] G.T. Barkema and N. Mousseau, Phys. Rev. Lett. **77**, 4358 (1996); R. L. C. Vink, G. T. Barkema, W. F. van der Weg, and N. Mousseau, J. Non. Cryst. Solid. (to be published).

[8] K. Laaziri, S. Kycia, S. Roorda, M. Chicoine, J.L. Robertson, J. Wang, and S.C. Moss, Phys. Rev. B **60**, 13 520 (1999).

[9] F. Wooten, K. Winer, and D. Weagire, Phys. Rev. Lett. **54**, 1392 (1985).

[10] A.A. Demkov, J. Ortega, O.F. Sankey, and M.P. Grumbach, Phys. Rev. B **52**, 1618 (1995).

[11] O.F. Sankey and D.J. Niklewski, Phys. Rev. B **40**, 3979 (1989).

[12] P. Stumm and D.A. Drabold, Phys. Rev. Lett. **79**, 677 (1997).

[13] D.A. Drabold, P.A. Fedders, and P. Stumm, Phys. Rev. B **49**, 16 415 (1994).

[14] M. Cobb and D.A. Drabold, Phys. Rev. B **56**, 3054 (1997).

[15] A. Szabo and N.S. Ostlund, *Modern Quantum Chemistry* (Dover, New York, 1996).

[16] N. Bernstein, M.J. Aziz, and E. Kaxiras, Phys. Rev. B **58**, 4579 (1998).

[17] E.P. Donovan, F. Spaepen, D. Turnbull, J.M. Poate, and D.C. Jacobson, J. Appl. Phys. **57**, 2782 (1985).

[18] D.A. Drabold, P.A. Fedders, S. Klemm, and O.F. Sankey, Phys. Rev. Lett. **67**, 2179 (1991).

[19] L. Ley, J. Reichardt, and R.L. Johnson, Phys. Rev. Lett. **49**, 1664 (1982).

[20] S.K. Bose, K. Winer, and O.K. Andersen, Phys. Rev. B **37**, 6262 (1988).

[21] D.K. Biegelsen and M. Stutzmann, Phys. Rev. B **33**, 3006 (1986).

[22] For a color version, see http://www.phy.ohiou.edu/~durandur/FIGURES/Fig3.jpg

[23] P.W. Anderson, Phys. Rev. **109**, 1492 (1958).